DIFFUSIVE AND CONVECTIVE DRYING ON A SHALY SANDSTONE USING NMR MEASUREMENTS

Y. Peysson, M. Fleury, F. Norrant andV. Blázquez Pascual[1]
Institut Français du Pétrole (IFP)

This paper was prepared for presentation at the International Symposium of the Society of Core Analysts held in Noordwijk, The Netherlands 27-30 September, 2009

ABSTRACT

Carbon capture and sequestration is one of the many solutions to reduce global warming. CO_2 can be injected in depleted oil and gas reservoirs or in aquifers and injection rates may be high due to a limited number of wells. In the near well bore region, super critical CO_2 is most likely in a dry state and not in thermodynamic equilibrium with the surrounding water. This may induce a decrease of the water content by drying even at irreducible saturation, followed by salt precipitation and potentially an alteration of the rock fabric, especially for shaly sandstone.

In this study, we investigated experimentally the drying rate on shaly sandstone in diffusive and convective conditions. In convective conditions as opposed to diffusive, air is injected at different flow rates through the porous media. We also varied the temperature from 30 up to 60°C, and the salinity from 50 up to 250 g/l to observe potential damage due to salt precipitation. The saturation profiles and water distribution in the pore network were monitored continuously using T_2 relaxation and 1D imaging NMR techniques.

For the range of temperature and air flow rate used, a drying front was never observed. Drying rate has a strong dependence on the temperature as predicted by Raoult law. The drying rates are enhanced largely with the air flow rate in convective conditions. Presence of salt has a more complex effect: an increase of the drying rate for high saturations but then a strong decrease for lower saturations.

INTRODUCTION

Geological sequestration of carbon dioxide can mitigate the climate global warming by limiting the accumulation of greenhouse gas in the atmosphere. The link between greenhouse gas increase and global warming is now established and the concentration of atmospheric carbon dioxide is the largest greenhouse gas contributor just after the water vapour. The injection of large quantities of CO_2 in aquifers or depleted reservoirs has been investigated for some years now and some large scale pioneer storage are currently in operation like in Sleipner, a formation located in the North Sea where Statoil disposes the carbon dioxide in a deep aquifer.

Dry gas injection at high rates in aquifers may lead to a large decrease of the water saturation around the well by evaporation. This may induce alteration of the

[1] Now with Laboratory of Petrophysics Madrid

permeability by salt precipitation. Drying of porous media induced by gas injection has been studied in the oil & gas industry because of water blocking problems [1] [2]. This phenomenon can appear for gas wells after injection of aqueous fluids during operations such as completion or workovers. The gas flow performance can be drastically reduced because of residual liquid saturation around the well. The presence of liquid decreases the gas return permeability.
Despite the alteration of the flow rate, gas slowly evaporates the water phase through drying and the initial gas flow performance is then restored. This effect has been studied theoretically and also experimentally in the framework of two phase Darcy flow by Mahadevan *et al.* recently [3] [4]. Water saturation evolution is evaluated taking into account gas flow rate, drying and capillary effects. Experiences with high and low permeability samples (Berea sandstones and Texas Cream limestone) were compared to the model [4]. The major effects are captured by the Darcy approach but some differences are still observed by the authors between the experiments and the model especially with the low permeability sample.
Convection driven drying has been investigated only very recently and few experimental studies are available in the literature. On the contrary, diffusion driven drying has been the object of a lot of studies and a complete overview can be found for example by Nadeau & Puiggali [5]. The decrease of water saturation is commonly divided into three stages [6]. A first one characterized by a quasi constant rate where the water saturation decreases quasi linearly with time. Then a first decreasing rate period where the continuity of the fluids in the porous media starts to break and finally a second decreasing rate period at very low rate.
In the context of CO_2 storage, some numerical simulations have been done with reservoir simulators to evaluate the extension of the drying zone in the near wellbore and to calculate the amount and distribution of salt precipitated [7-8]. But as mentioned by the authors, experimental work is needed to get a better understanding on drying rate and salt effects.

In this work, our objective was to investigate experimentally the evolution of the drying rate in convection and diffusion driven drying. Generally drying has been investigated by mass measurement with time in controlled temperature and outlet vapour saturation conditions. However convective driven drying requires a sample holder connected to a gas injection device. The mass measurement is then more difficult to handle. For this study a NMR technique was used to monitor in real time the water content in the sample with and without air flow through the porous media. The saturation profiles and water distribution in the pore network were monitored using T_2 relaxation and 1D imaging techniques.

EXPERIMENTAL SECTION

Experimental Set-up

We used a low field NMR instrument to follow the evolution of the amount of water present in the sample as a function of time, and to obtain semi-quantitative information concerning the saturation profiles. The NMR spectrometer is a MARAN 23.7 MHz from Oxford Instruments equipped with a 18 mm diameter probe and 1D imaging capabilities.

To characterize the sample in terms of pore size distribution and to follow the saturation profile, we used a non standard CPMG sequence with a variable inter-echo time. For the first echo, the inter echo time is set to 0.06 ms (an inter-pulse spacing of 0.03 ms), then it is increased up to 0.1 ms. Hence, we have a relaxation time resolution of about 0.06 ms and we are able to catch longer relaxation time with a reasonable number of pulses. The signal to noise ratio is usually greater than 100. To measure the saturation profile, we used a standard 1D imaging technique (a Hahn echo with a gradient encoding). The parameters of the sequence are such that the echo is generated at t=2 ms. Therefore, relaxation times smaller than 2 ms are weakly contributing to the signal intensity and the profiles are not quantitative in this range of relaxation times. In practice, a reference profile measured at $S_w = 1$ is first established and used to normalize the subsequent profiles measured during drying.

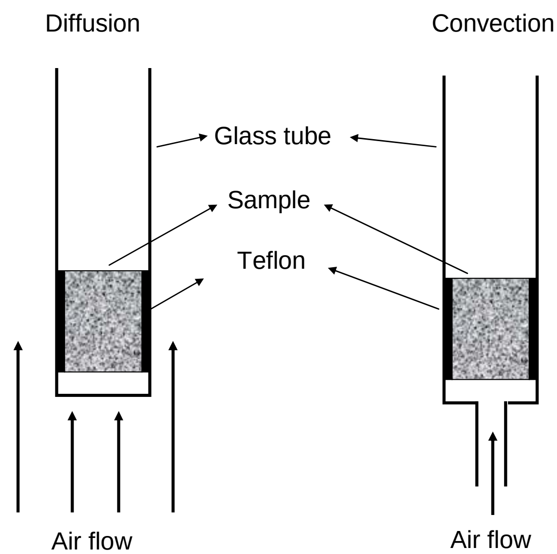

Figure 1: Schematic of the experimental set-up. The temperature of the air flow is regulated using the existing NMR set-up and the glass tube is placed inside the NMR magnet system regulated at 30°C. The temperature gradient at higher temperature is estimated to 1°C.

For diffusion driven drying, the sample is placed in a glass tube (Figure 1) with only the upper face open to the ambient air. The temperature is controlled by an air flux at a given temperature around the glass tube holder. In the case of convective driven drying, the air flow is injected at the bottom face, the lateral surface still being covered with Teflon. The air flow temperature is controlled similarly. Note that the NMR magnet is at 30°C. For higher temperatures, the temperature gradient along the sample is estimated at 1 °C due to the poor heat capacity of air. Acquisition is automatically performed at regular time intervals.

The water vapor concentration in the gas can be calculated at low pressure with Raoult law $C = P_s(T)/P$ where $P_s(T)$ is the vapor pressure of water and P the gas pressure. In a first approximation, C does not depend on the gas type. Hence, from this point of view, air instead of CO_2 can be used in the experiments to study drying for CO_2 storage applications.

Sample

In this study, we choose a Vosges Sandstone to represent a reservoir rock for CO_2 storage. All the experiments have been performed with a cylindrical plug with the dimensions of 14.5 mm in diameter and 21 mm in length. The measured gas (Air) permeability is 125 mD. The pore throat size distribution was measured through High Pressure Mercury Injection (Figure 2) and porosity was estimated at 21.8%.

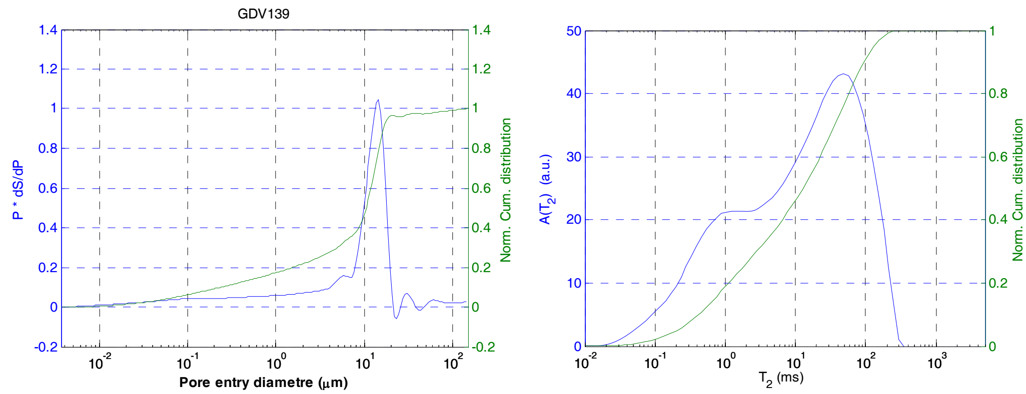

Figure 2 : Mercury pore throat size distribution and NMR pore size distribution of the Vosges sandstones sample used in the experiments. The porosity of the sample is 21.8% and the gas permeability is 125 mD.

This sandstone contains a relatively large amount of clays that are better easily detected by NMR. If we chose an arbitrary cut-off at T_2=3 ms (corresponding in this case to the saddle point in the NMR curve), the clay bound water would represent about 30% of the pore volume. From mercury injection, a cut off at d=2 μm yield a volume fraction of 20%. The same sample was used in all drying experiments. After complete drying, the plug is again saturated with NaCl brine and let at rest for a long period of time with a large brine volume in order to dissolve completely the salt previously precipitated.

EXPERIMENTAL RESULTS

Diffusive Drying

The NMR average water saturation in the plug was recorded as a function of time at 30°C, 45°C and 58°C (Figure 3). The average water saturation decreases regularly with time except for the very end of the drying process for the 3 temperatures investigated. We can also observe a residual saturation (Sw~0,04) that cannot be removed even if we continue flowing gas. This is discussed later. The effect of temperature on the time needed to dry the sample is very important. At 30°C it took 300 hours to obtain drying to residual saturation, but only 20 hours at 58°C.

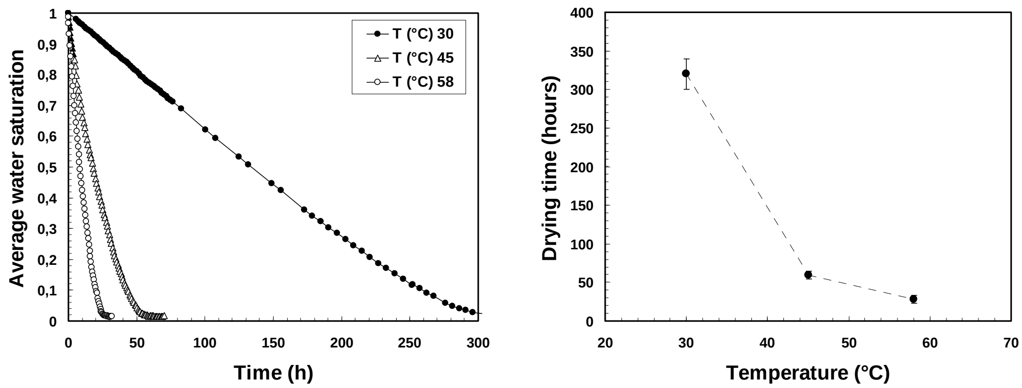

Figure 3 : Average water saturation evolution versus time at different temperature (30-45-58°C) in the diffusive regime and time necessary to total drying.

The relaxation time distributions give also interesting information on the water distribution in the pore network (Figure 4). The inter-granular pore water around 40 ms is evaporated first, followed by the clay bound water at larger time. At S_w = 20 %, the T_2 distribution contains components smaller than 10 ms characterizing only clay bound water. Finally, a new relaxation component appears at the end of drying and is interpreted as water trapped in clay interlayers. This water is not distinguished when the clays are saturated because it is in fast exchange with the surrounding water.

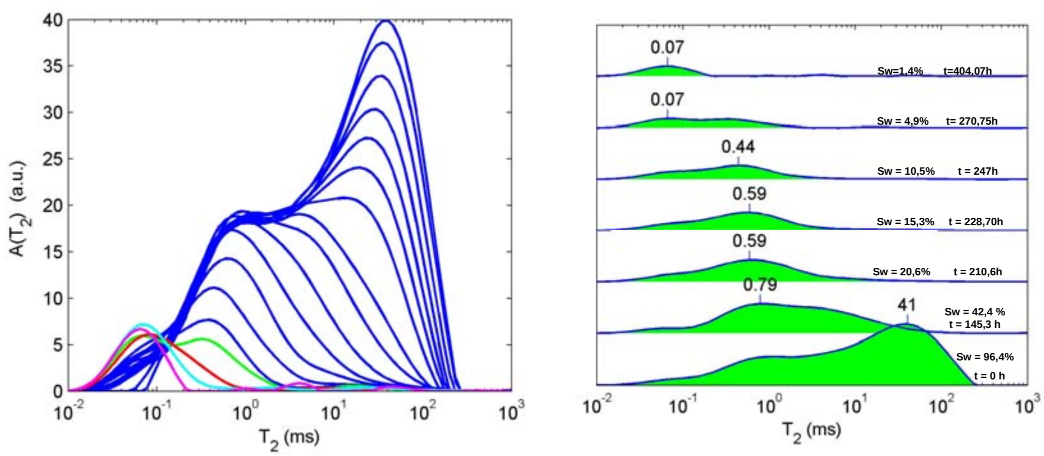

Figure 4 : T_2 time relaxation distributions versus time at 30°C in the diffusive regime. Left: superimposed graphs. Right: plot of some distributions.

The measured saturation profiles are uniform (Figure 5) and this observation confirms the absence of a drying front as also noted by some authors in the literature. Although drying may be more important at the upper face, the saturation gradient creates a water flux by capillarity. Water vapour in the sample is removed by a diffusive mechanism to the top of the sample. Because drying is slow, a classical assumption is that liquid and vapour are always locally at equilibrium in the sample [9] and so the vapour concentration is at the saturation concentration. There is no vapour accumulation at the upper face of the sample because it is displaced by convection and/or diffusion at the top of the glass tube.

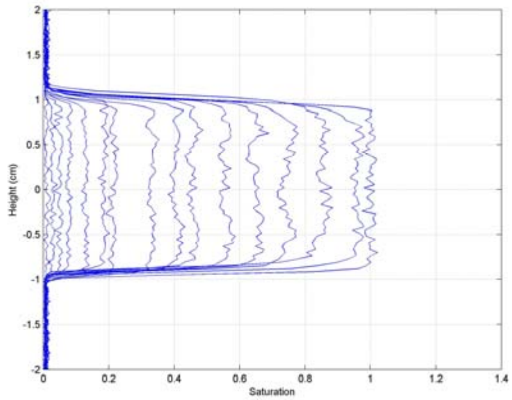

Figure 5 : Saturation profiles versus time at 30°C in the diffusive regime.

Convective Drying

Air is now injected through the sandstone plug at a temperature of 30°C. Injection of gas in the rock sample is expected to increase the drying rate. The sample is initially fully saturated with 30g/l NaCl brine and dried in the diffusive regime down to a saturation around 80-90% in order to have a gas relative permeability high enough to permit air flow without significant pressure drop. The average water saturation in the plug and saturation profiles were recorded with time at three different air flow rates.

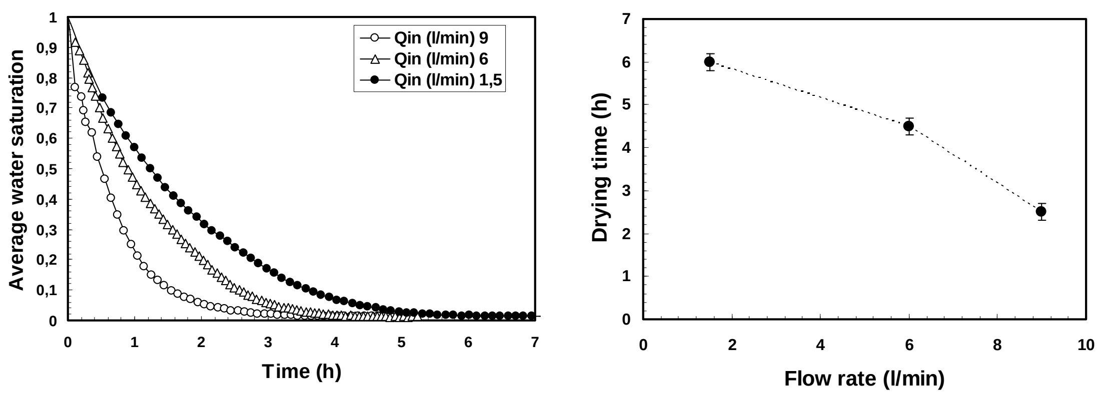

Figure 6 : Average water saturation evolution versus time at 30°C for 3 different air flows in the convective driven regime and time necessary to total drying.

In this configuration, the average water saturation decreases very rapidly: it took only a few hours to desaturate the sandstone. We still observe a residual saturation (S_w~0.04) that cannot be removed, certainly due to water in the clay interlayers.

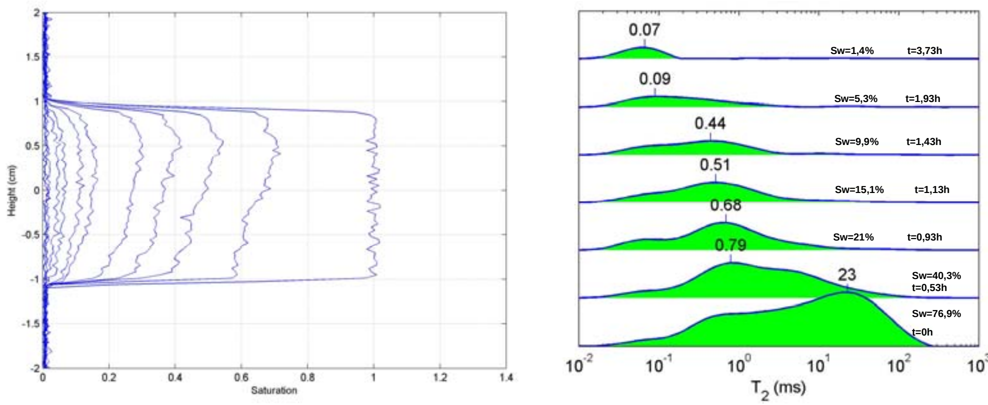

Figure 7 : Water saturation profiles and relaxation time distributions at the highest flow rate (9 l/min) and 30°C in the convective regime. The plug is vertical and the air flow from bottom to top.

The profiles are qualitatively slightly different from the diffusive driven regime (Figure 7). We clearly observe an increase of the saturation in the direction of the flow. This effect is due to a balance between the gas flow that push forward the water and the capillary forces that tends to flatten the profiles. This effect is more pronounced when the flow rate is higher, as expected. The evolution of the T_2 distribution (Figure 7) is however quite similar to the one in diffusive driven drying showing again that the largest pores are first dried. We observe again a remaining water quantity that is not removed.

DRYING RATE EVALUATION

Whatever the physical mechanisms used to evaporate the vapour phase from the porous media, diffusion or convection, we can define the rate at which vapour escapes the sample due to evaporation. This rate is the mass of vapour *M* that flow out of the sample by unit time and surface unit *A*:

$$V_d = \frac{1}{A}\frac{dM}{dt} \tag{1}$$

By mass balance, Coussot [6] states that the amount of water that escapes the sample through vapour is equal to the decrease of the water volume in the sample, so the drying rate can be related to the water desaturation rate:

$$V_d = -\frac{M_0}{A}\frac{dS}{dt} \tag{2}$$

where M_0 is the initial mass of water in the sample. So the measurement of the average saturation evolution with time is a way to assess experimentally the drying rate.

From our experimental results, we computed the drying rate and its evolution with the saturation in Figure 8 for the different situations studied using the relation (2).

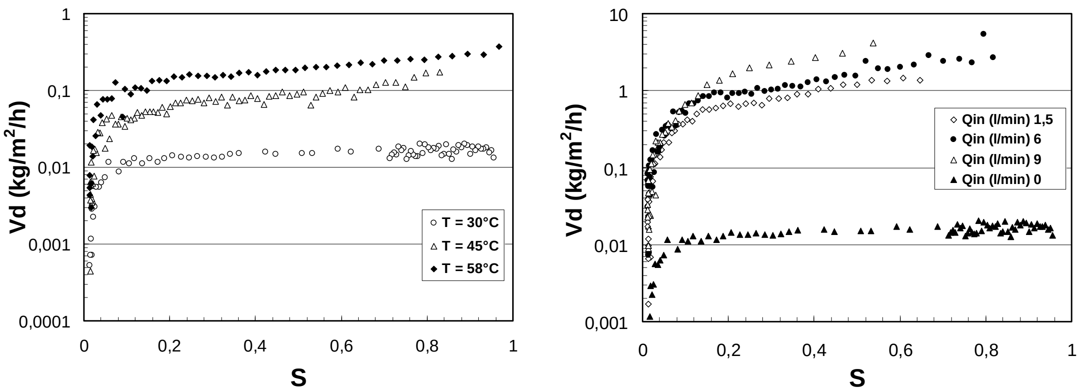

(a) (b)

Figure 8 : Drying rate $V_d = \frac{1}{A}\frac{dM}{dt}$ in kg/m^2/hour versus average saturation in the diffusive driven drying (a) for the 3 temperatures and convective driven drying (b) for the 3 air flow rates.

Diffusive Drying Rate

It is usually assumed that the diffusion driven drying regime starts with a constant rate period [6] [10]. We observe this constant rate period in our results but the rate is actually not strictly constant but there is a small decay until S_w ~ 0.2. The evaporation rate is compensated by the water flux due to the capillary forces. Coussot [6] also pointed out that he observed in his experimental results a slow decay period. At the end of this phase, the drying rate decreases strongly and finally goes to zero. The smallest pores sizes (clay) of the sample are desaturated in this regime

During the quasi constant period the drying rate is equal to the diffusive flux of water vapour:

$$V_d = \rho_v D \frac{\partial C}{\partial x} \approx \rho_v D \frac{C - C_0}{\delta} \quad (3)$$

where ρ_v is the vapour density, D is the vapour diffusion coefficient in the air, C the concentration of vapour in the air. Assuming that the vapour concentration is uniform in the sample, we can consider that the concentration gradient is located only at the top of the sample in a layer of thickness δ. The concentration gradient is related to the difference between C and C_0 the concentration outside the sample and δ [8]. Typically, D is of the order of 10^{-5} m^2/s, ρ_v is 1 kg/m^3, C is 10^{-3} at 30°C. If we take a millimetre for δ, we get $V_d \sim 10^{-2}$ kg/m^2/h which give a good order of magnitude for V_d.

With the evaluation of equation (3), we can also determine the variation of V_d with the temperature T (defined in Celcius degree). We assume the perfect gas law for air:

$$\rho_v / \rho_0 = \frac{T_{ref} + T_0}{T_{ref} + T}$$ (T_{ref} is 273.15°C to convert in Kelvin).

The gas diffusion coefficient variation with the temperature can be estimated from the kinetic theory of gases:

$$D/D_0 = \left(\frac{T_{ref} + T}{T_{ref} + T_0}\right)^{\frac{3}{2}}$$

and C can be estimated with the Raoult law:

$$C/C_0 = \left(\frac{T}{T_0}\right)^4.$$

In this last equation, the temperature is in Celsius because we use the Duperray correlation for the liquid-vapour saturation curve. Finally, the relative drying rate variation with the temperature is:

$$\frac{V_d}{V_d^0} \propto \left(\frac{T_{ref} + T}{T_{ref} + T_0}\right)^{\frac{3}{2}} \frac{T_{ref} + T_0}{T_{ref} + T}\left(\frac{T}{T_0}\right)^4 \quad (4)$$

This equation is actually very close to $\left(T/T_0\right)^4$.

From our experiment, we plot the drying rate in the first slow decreasing period relative to the drying rate at 30°C. This ratio does not depend on the value of the saturation, indeed, we observe that the three curves are homothetic. The relative drying rate is plotted versus T/T_0 in Figure 9 and equation (4) is also represented. We observe an excellent agreement between the experiment and the model.

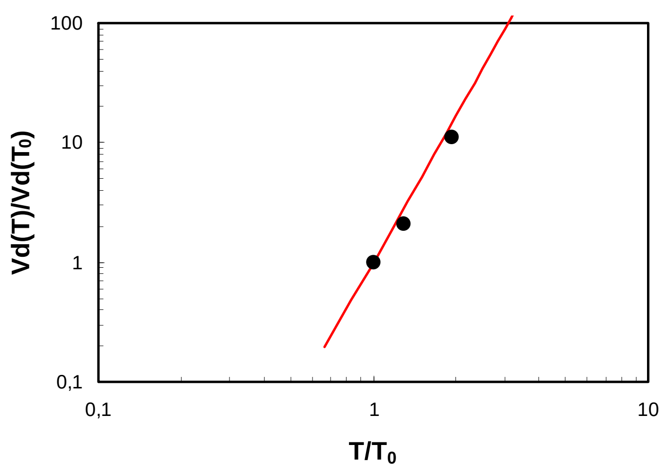

Figure 9 : Drying rate evolution with the temperature

Convective Drying Rate

In the first stage of the convective regime, we can consider that the evacuation of the vapour phase from the porous media is through the convection of the gas. So the drying rate is equal to the flux of water vapour:

$$V_d = \rho_v C U_g \quad (5)$$

Here again, we can estimate the order of magnitude of the drying rate. Taking ρ_v as 1 kg/m^3, C is 10^{-3} at 30°C and Q_g = 1 l/min, we get V_d ~ 1 kg/m^2/h which is in good agreement with the observation. We can also check the linear evolution of the drying rate with the gas velocity. For S_w = 0.6, we plot the drying rate evolution with the imposed air flux in Figure 10. The linear adjustment of the measurement is only roughly satisfied.

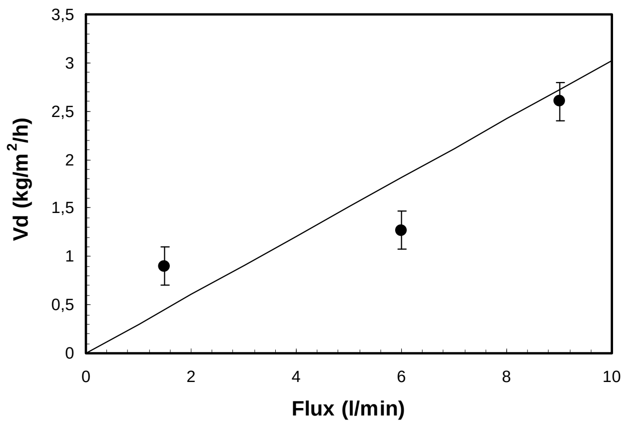

Figure 10 : Drying rate measured for S_w=0.6 for the three imposed air flow rates. The black line is a linear adjustment.

In our experiments, we do not observe a plateau for the drying rate at imposed air flow rates, because as the samples dry, the gas permeability changes and the pressure at the inlet decreases. Therefore the volumetric mass of the gas decreases as does the drying rate. The dynamic drying rate is then more complex and this effect lasts until S_w = 0.2. For lower saturations, the drying rate drops rapidly, and the remaining water is more difficult to evaporate.

EFFECTS OF SALT

We study also the effect of salt concentration on the drying rate. The sandstone sample was prepared with high NaCl initial concentrations, C_i = 250 and C_i = 300 g/l in order to induce salt precipitation. The average water saturation was then measured at 58°C without any flow trough the rock. The drying rate is deduced and represented in Figure 11.

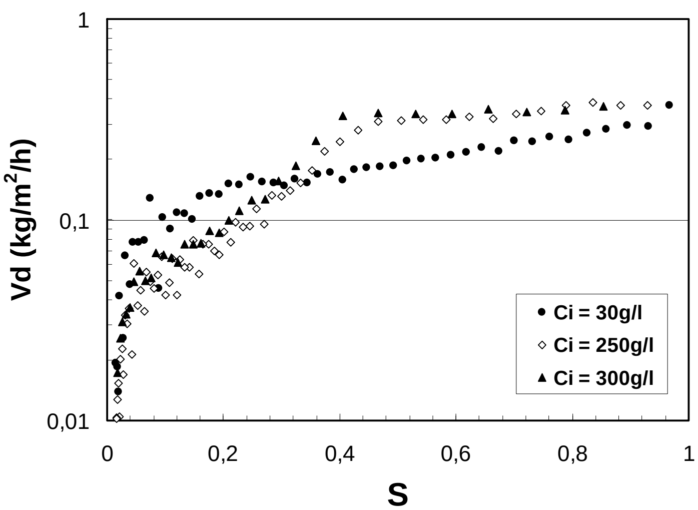

Figure 11 : Drying rate in kg/m^2/hour versus average saturation in the diffusive driven drying regime for three initial NaCl concentrations.

The experimental results shown in Figure 11 are surprising. Indeed, thermodynamically the presence of salt decreases the vapour concentration, so the diffusive flux should be smaller in this case and we measure a drying rate clearly higher for C_i = 250 and 300g/l than for C_i = 30g/l. This effect has been also observed by Sghair in his PhD work [11] and he explained this observation by the efflorescence of the salt. This mechanism is the growth of salt crystals on the outside the plug that imbibes out water due to capillary forces. In this range of large salt concentrations we do observe a deposition of salt outside of the sample. But this means that salt precipitation starts very early which is quite unexpected.

Another observation is the sudden decrease of the drying rate at S_w = 0,45. The NaCl critical salt concentration is 356g/l. This concentration is reached at S_w =0,70 for C_i = 250 g/l and S_w =0,84 for C_i = 300 g/l. So, in the first stage of drying, the salt precipitation does not modify significantly the evolution of the drying rate. But when a certain amount of salt has been precipitated, the drying rates are reduced. Water may be trapped in microporosity formed by halite crystals and therefore modify the drying rate. However, after final drying, no water is left except the clay interlayer residual water described above.

CONCLUSION

In this study, we investigated experimentally the drying rate on a shaly sandstone in diffusive and convective conditions. The average saturation, the pore size distribution and saturation profiles are followed by NMR. In convective conditions as opposed to diffusive, the normalized drying rate is about 10 times larger. The temperature has a large impact and increases the drying rate according to an expected power law involving an exponent 4. The gas flow rate is expected to have a linear effect on the drying but this needs more investigation. In the diffusive regime, salt crystallization does not strongly impact the drying rate but the experiments are influenced by perturbing boundary conditions (efflorescence). The new observation is that the drying rate is much smaller in the clays than in the inter-granular pores.

REFERENCES

1. Kamath, J., Laroche C., 2003 "Laboratory-Based evaluation of gas well deliverability loss caused by water blocking", SPE Journal March 2003) p71-80.
2. Parekh B., Sharma M.M., 2004"Cleanup of water blocks in depleted low-permeability reservoirs", SPE paper 89837 presented at SPE ATCE 2004 Texas USA.
3. Mahadevan J., Sharma M.M., Yortsos Y.C., 2006, "Flow-Through drying of porous media", AIChE Journal, Vol 52, N°7, p2367-2380 .
4. Mahadevan J., Sharma M.M., Yortsos Y.C., 2007, "Water removal from porous media by gas injection : experiments and simulation", Trans. Porous Med., Vol 66, p287-309.
5. Nadeau J.P., Puiggali J.R. 1995 "Drying – From physical to industrial processes", Tec&Doc Lavoisier Paris (In french).
6. Coussot P. 2000 "Scaling approach of the convective drying of a porous medium", Eur. Phys. J. B. vol 15, 557-566.
7. Hurter S., Labregère D., Berge J. 2007 "Simulation for CO_2 injection projects with compsitional simulator" SPE Paper 108540.
8. Muller N., Qi R. Mackie E, Pruess K. Blunt M.J. 2008, "CO_2 injection impairment due to halite precipitation" Proceeding of the GHGT-9 conference, Washington 2008.
9. Puiggali J.R., Quintard M., 1992, "Properties and simplifying assumptions for classical drying models", Advances in Drying, Chapter 4, Hemisphere publishing.
10. Sghaier N., Prat M., Ben Nasrallah S. 2007 "On ions transport during drying in a porous medium", Transp. Porous. Med Vol 67 p243-274
11. Sghaier N., 2006 "Drying in porous media with dissolved salt –Influence of liquid films and wetting properties", PhD report.